RNA-directed DNA methylation induces transcriptional activation in plants

Kenichi Shibuya[1], Setsuko Fukushima, and Hiroshi Takatsuji[2]

Plant Disease Resistance Research Unit, Division of Plant Sciences, National Institute of Agrobiological Sciences, Tsukuba 305-8602, Japan.

Edited by David Baulcombe, University of Cambridge, Cambridge, United Kingdom, and approved December 9, 2008 (received for review September 17, 2008)

A class-C floral homeotic gene of *Petunia*, *pMADS3*, is specifically expressed in the stamen and carpels of developing flowers. We had previously reported the ect-*pMADS3* phenomenon in which introduction of a part of the *pMADS3* genomic sequence, including intron 2, induces ectopic expression of endogenous *pMADS3*. Unlike transcriptional or posttranscriptional gene silencing triggered by the introduction of homologous sequences, this observation is unique in that the gene expression is up-regulated. In this study, we demonstrated that the ect-*pMADS3* phenomenon is due to transcriptional activation based on RNA-directed DNA methylation (RdDM) occurring in a particular CG in a putative *cis*-element in *pMADS3* intron 2. The CG methylation was maintained over generations, along with *pMADS3* ectopic expression, even in the absence of RNA triggers. These results demonstrate a previously undescribed transcriptional regulatory mechanism that could lead to the generation of a transcriptionally active epiallele, thereby contributing to plant evolution. Our results also reveal a putative negative *cis*-element for organ-specific transcriptional regulation of class-C floral homeotic genes, which could be difficult to identify by other approaches.

epiallele | flower | MADS-box | petunia | RdDM

DNA methylation and histone modifications have been implicated in many biological processes including transcriptional gene silencing (TGS), genome imprinting, and paramutation in plants and animals. In many instances, RNA molecules play a crucial role as a trigger to induce a series of reactions leading to the modulation of gene expression mediated by DNA methylation and/or histone modifications. Small double-stranded RNAs (dsRNAs) of 21–24 bp trigger RNA-directed DNA methylation (RdDM) of homologous DNA sequences, leading to TGS in plants (1, 2). Induction of TGS by small RNAs has also been reported in human cells (3, 4). Involvement of dsRNAs due to RNA-dependent RNA polymerase (RdRP) and possibly small RNAs has been shown in paramutation of the *b1* locus in maize (5, 6). These epigenetic regulations reported so far have been the down-regulation of transcription. Recently, however, 2 research groups have reported that the addition of small dsRNAs homologous to transcriptional regulatory sequences of certain endogenous genes up-regulates the transcription of target genes in human cultured cells (7, 8). This finding is striking because it has shown the existence of a previously undescribed type of small dsRNA-mediated regulation, a regulation opposite to that of TGS. However, only limited numbers of observations have been reported and their underlying mechanisms are still unclear.

We had previously reported that the introduction of a part of the genomic sequence of *pMADS3*, a class-C floral homeotic gene, induces ectopic up-regulation of endogenous *pMADS3* in the flowering plant *Petunia hybrida* (9). This gene is a petunia ortholog of *AGAMOUS* (*AG*), an Arabidopsis class-C floral homeotic gene involved in the specification of stamens and carpels (10). *AG* contains a long second intron (intron 2), which contains a regulatory sequence that is sufficient for stamen- and carpel-specific expression (11–13). Several regulatory factors that positively or negatively control *AG* expression through interaction with intron 2 have been identified (12, 14–17). In our previous research, we introduced a chimeric gene, *pMADS3:GUS*, in which the genomic sequence of *pMADS3* including its upstream and intragenic sequence up to intron 2 was fused with the coding sequence of the β-glucuronidase gene (*GUS*), into petunia lines. This transgene induced an unexpected homeotic conversion of floral organs due to disturbed expression of endogenous *pMADS3*. In some transgenic lines, *pMADS3* expression was silenced, accompanied by conversion of stamens into carpels. In other lines, endogenous *pMADS3* was ectopically up-regulated in petals, sepals, and leaves resulting in floral homeotic changes and curled leaves, which were unpredictable outcomes. In *pMADS3:GUS* plants, the 2 homeotic phenotypes—due to silencing and ectopic expression of endogenous *pMADS3*—interconverted somatically during development and were inherited independently of the transgenes. Aberrant RNAs, including sense and antisense sequences of *pMADS3* intron 2, were detected in these transformants. On the basis of these findings, we speculated that an epigenetic regulatory mechanism, presumably involving trigger RNAs and DNA methylation, underlies this unique phenomenon (the ect-*pMADS3* phenomenon).

In this study, we investigated the molecular mechanism underlying the ect-*pMADS3* phenomenon. We showed that the ect-*pMADS3* phenotype was reproduced by expressing inverted repeat (IR) sequences for subregions of *pMADS3* intron 2 in transformant petunia lines. Then, we demonstrated that DNA methylation at specific CGs within the region targeted by IR in intron 2 is correlated with the ectopic up-regulation of *pMADS3*, leading to the conclusion that RdDM in particular regulatory sequences can induce transcriptional up-regulation. This acquired trait—due to transgene introduction—was inherited by the T_1 generation independent of transgenes, suggesting a mechanism to generate a transcriptionally active epiallele. In addition, our findings fortuitously suggested a previously uncharacterized negative *cis*-element for spatiotemporal expression of class-C floral homeotic genes.

Results

Induction of *pMADS3* Ectopic Expression by Expressing IR Sequences for *pMADS3* Intron 2. Our previous studies had showed that transgene-dependent expression of *pMADS3* transcripts, including sense and antisense sequences of *pMADS3* intron 2, was

Author contributions: K.S. and H.T. designed research; K.S. and S.F. performed research; K.S., S.F., and H.T. analyzed data; and K.S. and H.T. wrote the paper.

The authors declare no conflict of interest.

This article is a PNAS Direct Submission.

Freely available online through the PNAS open access option.

[1]Present address: National Institute of Floricultural Science, National Agriculture and Food Research Organization (NARO), Tsukuba 305-8519, Japan.

[2]To whom correspondence should be addressed. E-mail: takatsuh@affrc.go.jp.

This article contains supporting information online at www.pnas.org/cgi/content/full/0809294106/DCSupplemental.

strongly correlated with the ect-*pMADS3* phenotype in *pMADS3*:*GUS* transformant petunia lines. On the basis of this observation, we suggested the involvement of dsRNAs in this phenomenon (9), similar to the previous report of the silencing of *chalcone synthase* in petunia lines (18, 19). It has been shown that the expression of transcripts coding for IR sequences can result in the production of small dsRNAs through an RNA processing (RNAi) mechanism, and the small dsRNAs guide DNA methylation to homologous DNA sequences (i.e., RdDM), eventually leading to TGS (2). To test the hypothesis that an RdDM-like mechanism is involved in the ect-*pMADS3* phenomenon, we expressed IR sequences for a subregion of *pMADS3* intron 2 to see whether expressed RNAs induce the ect-*pMADS3* phenotype. We first targeted 1-kb subregions of *pMADS3* intron 2 (4 kb) by expressing corresponding IR sequences. Transformants of V002 lines expressing IR sequences corresponding to nucleotides (nts) 1001–2000 (with the first nucleotide of intron 2 as nt 1) frequently showed homeotic changes with staminoid structures developed at the margins of petal limbs and along the midveins (ect-*pMADS3* flower phenotype) (Fig. 1 *A* and *B*). Quantitative PCR analyses showed that endogenous *pMADS3* was expressed ectopically in petals in these plants (Fig. 1*C*). No homeotic change was observed in other lines expressing IR sequences corresponding to nts 1–1000, 2001–3000, and 3001–4010 (Fig. 1*A*). These results indicate that the 1001–2000 region includes sequences responsible for the ect-*pMADS3* phenotype. Then, we targeted smaller subregions of the 1001–2000 region by IR sequences (lines V005–V010). Among the transformants, those of V008 lines, in which nts 1501–1800 were targeted, frequently showed the ect-*pMADS3* phenotype (Fig. 1*A*). Further dissection of the 1501–1800 region showed that transformants expressing IR sequences that include the 1701–1800 (V008, V009, V016, and V019) region displayed strong ect-*pMADS3* phenotypes at high frequencies (Fig. 1*A*). The ect-*pMADS3* phenotype was not observed in transformants of V018 and V010 lines in which neighboring 1601–1700 and 1801–2050 regions, respectively, were targeted. Interestingly, the ect-*pMADS3* phenotype became stronger with shorter target sequences. In V016 and V019 plants, in which the 1601–1800 and 1701–1800 regions were targeted, respectively, high levels of *pMADS3* expression were also induced in sepals and leaves in addition to petals, accompanied by strong homeotic changes, including staminoid petals and curled leaves (Fig. 1 *B* and *C*). These results indicate that the 1701–1800 region in *pMADS3* intron 2 is critical for the induction of *pMADS3* ectopic expression.

DNA Methylation in *pMADS3* Intron 2 Is Correlated with *pMADS3* Ectopic Expression. It is known that small dsRNAs resulting from expressed IR sequences can trigger RdDM to homologous DNA sequences in plants (2). We detected small dsRNAs including the sequences corresponding to expressed IR sequences in V019 plants showing the ect-*pMADS3* phenotype (supporting information (SI) Fig. S1). Therefore, we analyzed the DNA methylation status in the 1701–1800 region with bisulfite sequencing by using genomic DNA from petals. In wild-type petunia plants, no cytosine methylation was detected; in contrast, cytosines in all of the CG, CNG, and CNN contexts were found to be methylated in IR-targeted sequences of the transformants (Fig. 2). These results indicate that the expressed IR sequences induced *de novo* RdDM. In general, cytosines in symmetric sites (CG and CNG) were more heavily methylated than those in asymmetric sites (CNN) (Fig. 2). In V016 and V019 plants showing strong ectopic expression of *pMADS3*, cytosines in the 1701–1800 region were heavily methylated. In contrast, in lines that did not show the ect-*pMADS3* phenotype (e.g., V010 and V018), cytosine methylation was detected in IR-targeted sequences but not in the 1701–1800 region. Thus, DNA methylation at the 1701–1800 region of *pMADS3* intron 2 is strongly correlated with *pMADS3* ectopic expression.

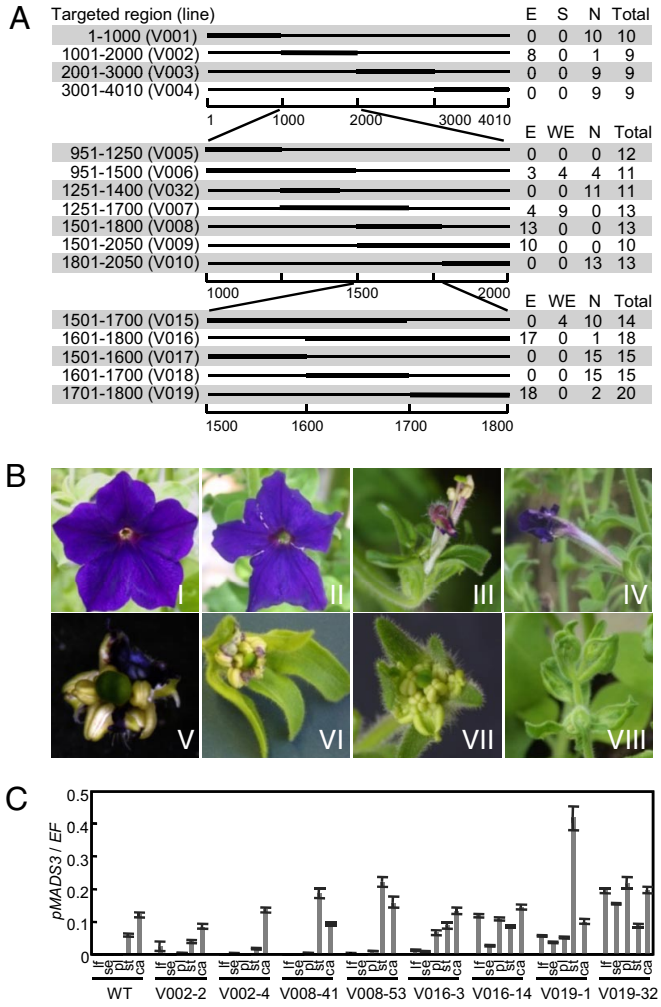

Fig. 1. Targeting of *pMADS3* intron 2 subregions by inverted repeat (IR) sequences. (*A*) Diagrams for target regions of IR expression in *pMADS3* intron 2. Scales represent nucleotide numbers with the first nucleotide of *pMADS3* intron 2 as nt 1. To the right are the numbers of transformant lines showing ect-*pMADS3* (E), weak ect-*pMADS3* (WE), *pMADS3* silencing (S), and normal (N) phenotypes (9). (*B*) Flower phenotypes of transformant plants expressing IRs. (*Bi*) A flower of wild-type petunia (V26); (*Bii*) a typical flower of V002 plants showing the ect-*pMADS3* phenotype with antheroid sectors along midveins and reduced petal limbs; flowers of V016 (*Biii*) and V019 (*Biv*) plants showing ect-*pMADS3* phenotypes with antheroid tissues on petal limbs; (*Bv*) a flower of V019 plants showing strong ect-*pMADS3* phenotype with antheroid petals (some flowers showed strong phenotypes as shown but others in the same plants showed milder ones); (*Bvi*) a typical flower of V034 plants showing strong ect-*pMADS3* phenotype with petal-to-anther conversion; (*Bvii*) extreme flower phenotype of 71–14 × M (T_1) showing complete conversion of petals to anthers; and (*Bviii*) curled cauline leaves of the V019 line. (*C*) Levels of *pMADS3* transcripts in leaves (lf), sepals (se), petals (pl), stamens (st), and carpels (ca) of transgenic lines. Expression levels of *pMADS3* relative to those of the elongation factor gene (*EF*) were measured by RT-qPCR. Mean ± SE ($n = 3$).

These results prompted us to examine whether DNA methylation in the same sequence region is also involved in the ect-*pMADS3* phenotype of *pMADS3*:*GUS* lines, in which we had originally observed this phenotype. In some *pMADS3*:*GUS* lines, the ect-*pMADS3* phenotype was maintained in the T_1 generation even after the transgene had segregated away (9). The presence of transgenes hampers DNA methylation analysis because they

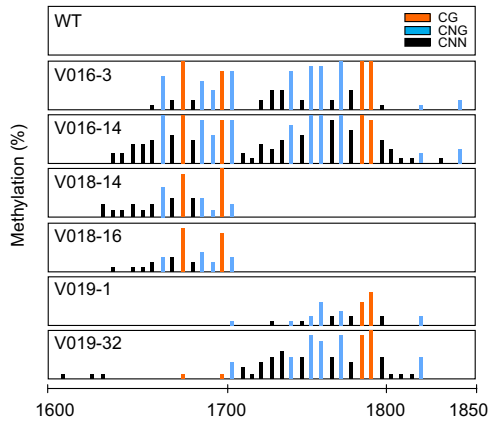

Fig. 2. DNA methylation patterns in *pMADS3* intron 2 of inverted repeat (IR)-expressed transgenic plants. V016 and V019 plants show the ect-*MADS3* phenotype, whereas V018 plants show normal phenotypes. At least 9 clones are sequenced for each bisulfite-treated sample. Bars represent proportions of methylated clones at each site; red, blue, and black bars represent CG, CNG, and CNN sites, respectively. The scale represents nucleotide numbers in *pMADS3* intron 2 with the first nucleotide of intron 2 as nt 1.

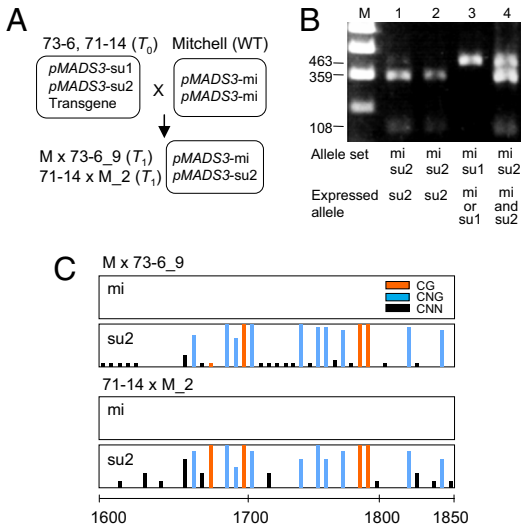

Fig. 3. DNA methylation patterns in outcrossed *pMADS3*:*GUS* plants. (*A*) Inheritance of individual *pMADS3* alleles in the T_1 generation. Transgenes segregated out in both M × 73-6_9 and 71-14 × M_2 plants showing the ect-*pMADS3* phenotype. (*B*) Allele-specific expression of endogenous *pMADS3* in the petals of *pMADS3*:*GUS* T_1 plants. The transformants analyzed were those without transgenes showing the ect-*pMADS3* phenotype. The allele-specific expression was analyzed as described previously (9). M: marker; lane 1: 71-14 × M_2; lane 2: M × 73-6_9; lane 3: M × 73-6_7; lane 4: 71-14 × M_11. (*C*) DNA methylation patterns in *pMADS3*-mi and *pMADS3*-su2 alleles of M × 73-6_9 and 71-14 × M_2 plants. Bars represent proportions of methylated clones at each site; red, blue, and black bars represent CG, CNG, and CNN sites, respectively. The scale represents nucleotide numbers in *pMADS3* intron 2 with the first nucleotide of intron 2 as nt 1.

are usually indistinguishable from their corresponding endogenous gene in DNA sequences. However, the lack of a *pMADS3* transgene enabled DNA methylation analysis of these T_1 plants. Moreover, *pMADS3*:*GUS* plants have a genetic background of a F_1 hybrid (Surfinia); therefore, slight differences in the DNA sequences between 2 *pMADS3* alleles (*pMADS3*-su1 and *pMADS3*-su2) allowed us to analyze the expression and DNA methylation patterns of the individual *pMADS3* alleles (9). We crossed T_0 transformants of 2 *pMADS3*:*GUS* lines (73–6 and 71–14), having *pMADS3*-su1 and *pMADS3*-su2 alleles in addition to the *pMADS3*:*GUS* transgene, with a pure variety of *P. hybrida* cv. Mitchell having a *pMADS3*-mi allele (Fig. 3*A*). From among the T_1 offspring obtained, 2 plants (M × 73-6_9 and 71-14 × M_2) having *pMADS3*-su2 and *pMADS3*-mi alleles but not the transgenes were selected and analyzed for DNA methylation. Both plants inherited *pMADS3*-su2 and *pMADS3*-mi alleles from their parent *pMADS3*:*GUS* and Mitchell plants, respectively, but only the *pMADS3*-su2 allele was preferentially expressed in the petals of both plants (Fig. 3*B*). Bisulfite sequence analysis revealed high levels of CG and/or CNG methylation and negligible levels of CNN methylation in the 1701–1800 region of the *pMADS3*-su2 allele (Fig. 3*C*). In contrast, no cytosine methylation in any sequence context was detected in the *pMADS3*-mi allele (Fig. 3*C*). These results further support the correlation between the CG and/or CNG methylation in this region and the ect-*pMADS3* phenotype, and also indicate that the effects of DNA methylation in *pMADS3* intron 2 act only in *cis* because only the methylated allele was up-regulated. We also detected small dsRNAs corresponding to the 1701–1800 sequence in the T_0 transformants of *pMADS3*:*GUS* lines (Fig. S1), indicating that basically common mechanisms are involved in the induction of ect-*pMADS3* phenotypes of *pMADS3*:*GUS* and IR-expressed lines.

Recent studies have highlighted the roles of chromatin remodeling via histone modification in transcriptional regulation. In both plants and mammals, DNA methylation is often associated with histone modification (H3K9me) (20, 21). In Arabidopsis, H3K27 trimethylation by CURLY LEAF (CLF), a polycomb-group protein, has been implicated in the transcriptional repression of *AG* (22). Therefore, we examined whether histone modification is involved in the ect-*pMADS3* phenomenon in addition to DNA methylation. In the transformant line (V016) showing *pMADS3* ectopic expression, H3K4me3 and H3K27me3 were detected in the 1601–1800 IR-targeted region but at similar levels to that in the wild type (WT) (Fig. S2). Acetyl-H3, H3K9me2, H3K27me1, and H3K36me2, which are often associated with transcriptional regulation, were not detected in either WT or V016 plants (Fig. S2). These results suggest that *pMADS3* ectopic expression is a direct consequence of DNA methylation rather than that mediated by histone modification.

Candidate *cis*-Element Responsible for RdDM-Induced Up-Regulation of *pMADS3*. The 1701–1800 region responsible for *pMADS3* ectopic expression contains 2 CG and 5 CNG sites. To identify the specific cytosine(s) responsible for the ect-*pMADS3* phenotype, we further dissected the 1701–1800 sequence by expressing IRs for its subregions. This region contains a 53-bp sequence (nts 1712–1764) including 2 CCAATCA boxes that are highly conserved in several plant species, as revealed by shadowing and footprinting analyses (23) (Fig. S3). We focused on these sequences and expressed IR sequences containing the 2 CCAATCA boxes (nts 1601–1767; V033) and the region downstream of them (nts 1768–1900; V034). In both V033 and V034 plants, we observed ectopic expression of endogenous *pMADS3* in petals (Fig. 4*B*). In all of the V033 plants examined, we detected methylation at all of the CG and CNG sites in the IR-targeted region (nts 1601–1767) (Fig. 4*A*). In addition, 2 CG sites at nts 1768 and 1771 immediately downstream of the targeted region were also methylated in these plants. These methylations are presumably due to a mechanism related to transitive silencing in which RNA silencing spreads outside target regions in both 3′ and 5′ directions in plants (24). In V034 plants, cytosines in the IR-targeted region including the 2 CG sites at nts 1768 and 1771 were methylated. In the V034–9 plant, only the 2 CG sites at nts 1768 and 1771 were methylated within

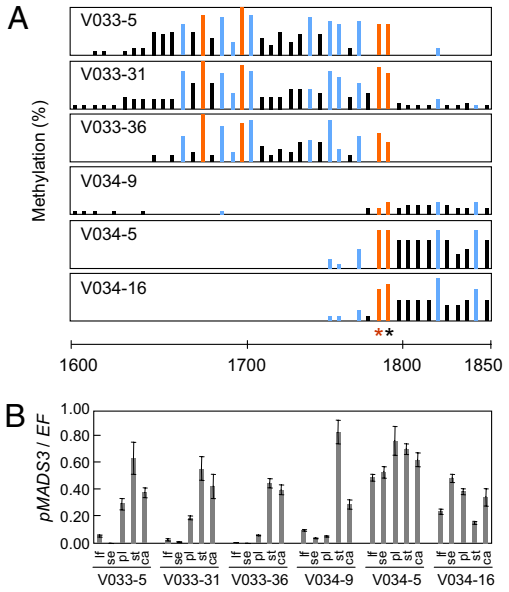

Fig. 4. DNA methylation patterns and *pMADS3* expression in V033 and V034 plants. (*A*) DNA methylation patterns in the 1600–1850 region. Bars represent proportions of methylated clones at each site; red, blue, and black bars represent CG, CNG, and CNN sites, respectively. The scale represents nucleotide numbers in *pMADS3* intron 2 with the first nucleotide of intron 2 as nt 1. Asterisks indicate CG sites at nts 1768 (red) and 1771 (black). (*B*) *pMADS3* mRNA levels in leaves (lf), sepals (se), petals (pl), stamens (st), and carpels (ca) of transgenic lines. Expression levels of *pMADS3* relative to those of the elongation factor gene (*EF*) were measured by RT-qPCR. Mean ± SE ($n = 3$).

the 1701–1800 region (Fig. 4*A*), besides a CNN methylation (nt 1766) that is unlikely to be responsible for the phenotype (see previous discussion). This plant still showed *pMADS3* ectopic expression, although weakly (Fig. 4*B*). Taken together, the 2 CG sites at nts 1768 and 1771 were the only sites that were commonly methylated in all of the transformants showing the ect-*pMADS3* phenotype. These results strongly suggest that methylation of the CGs at nts 1768 and/or 1771 is responsible for *pMADS3* ectopic expression.

We aligned the sequences corresponding to the 1701–1800 region of *pMADS3* intron 2 in 15 *AG* orthologs of 13 plant species belonging to 9 different families (Table S1). This alignment allowed us to find a highly conserved region immediately downstream of the 2 CCAATCA boxes (Fig. 5 and Fig. S3). Notably, the CG at nt 1768, 1 of the 2 CGs (nts 1768 and 1771) correlated with *pMADS3* ectopic expression, is within this region and was perfectly conserved in all of the plant species examined. The sequence surrounding this CG, TAGCTC*G*A, was also highly conserved among the plant species, suggesting that this sequence motif is a *cis*-element that plays a role in transcriptional regulation of *pMADS3*. In an attempt to functionally characterize the TAGCTC*G*A motif as a *cis*-element, we fused the entire 4-kb sequence of *pMADS3* intron 2 upstream of the *CaMV 35S* minimal promoter connected to the *GUS* reporter gene, as reported for Arabidopsis *AG* (12). Unfortunately, however, this construct gave no *GUS* activity in transgenic petunia lines for unknown reasons; therefore, we were unable to characterize the in vivo activity of this motif as a *cis*-element.

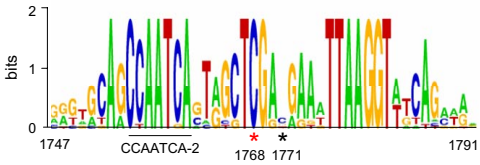

Fig. 5. Sequence logo for conserved motifs in the intron 2 of *pMADS3* homologs. The sequence logo (created by weblogo.berkeley.edu) was generated from 15 *pMADS3* homologs of 13 plant species belonging to 9 different families (see Table S1). Asterisks indicate CG sites at nts 1768 (red) and 1771 (black). Numbers at the bottom indicate the positions in *pMADS3* intron 2.

Discussion

On the basis of the unexpected expression patterns of endogenous *pMADS3* incidentally observed in *pMADS3*:*GUS* transgenic petunia plants, we characterized the molecular mechanism underlying this epigenetic phenomenon. The accumulation of aberrant transcripts including sense and antisense sequences for *pMADS3* intron 2 in the transformants (9) led us to speculate that the aberrant transcripts may have triggered the disturbance of endogenous *pMADS3* expression. To prove this hypothesis and further investigate the underlying molecular mechanisms, we expressed IR sequences for *pMADS3* intron 2, demonstrating that the expression of the IR sequences did induce the ect-*pMADS3* phenotype. Small dsRNAs for *pMADS3* intron 2 were detected in both *pMADS3*:*GUS* and IR-targeted transformants showing *pMADS3* ectopic expression. Moreover, we found that DNA methylation of a particular CG was strongly correlated with *pMADS3* ectopic expression in both transformants. On the basis of these observations, we propose the following mechanism for the ect-*pMADS3* phenomenon occurred in *pMADS3*:*GUS* transformants: transgene-derived aberrant transcripts including *pMADS3* intron 2 sequences were converted into dsRNAs by a reaction such as RdRP reaction and dsRNAs were processed into small dsRNAs, which triggered RdDM in their homologous DNA sequences in endogenous *pMADS3*, leading to the induction of its ectopic expression. We have not provided more direct evidence for the involvement of RdDM by using RNAi pathway mutants, such as the *Dicer* mutant; however, this model seems to be quite reasonable considering generally accepted outcomes resulting from the expression of IR constructs into plants.

Several reports have shown that DNA methylation in transcriptional regulatory regions is associated with gene silencing (TGS) in plants and mammals (25, 26). Deng *et al.* (27) provided evidence that DNA methylation within, or near sequences of, a positive *cis*-element (enhancer) interferes with the binding of a cognate transcription factor to this *cis*-element, which in turn causes TGS. The *pMADS3* silencing observed in some *pMADS3*:*GUS* lines is presumably due to this mechanism (9, 28). A mechanism analogous to this can account for the up-regulation of *pMADS3* in the ect-*pMADS3* phenomenon. If DNA methylation occurs in a negative *cis*-element (silencer), instead of a positive *cis*-element (enhancer), the binding of its cognate transcriptional repressor to this *cis*-element would be interfered with, leading to derepression of transcription. So far, such regulation has been reported for *Igf2*, an imprinted gene in mice. CG methylation in a negative regulatory sequence of *Igf2* derepressed this gene by interfering with the binding of a transcriptional repressor GCF2 to the sequence (29, 30).

Detailed dissection of *pMADS3* intron 2 by IR expression followed by DNA methylation analysis revealed a specific CG, the methylation of which is strongly correlated with the up-regulation of *pMADS3* transcription. This CG is located within the TAGCTC*G*A motif that is highly conserved among *AG* orthologs in various plant species. Taken together, this sequence motif is most likely a negative *cis*-element involved in spatio-temporal transcriptional regulation of *pMADS3*, and CG methylation within this motif presumably interferes with the binding of its cognate transcriptional repressor, leading to transcriptional derepression of *pMADS3*. Spatiotemporal regulation of the transcription of class-C floral homeotic genes has been extensively investigated as a model system to study floral-organ

PLANT BIOLOGY

specification. Our finding of a putative negative *cis*-element for *pMADS3* transcription may shed light on the regulation of class-C genes. In Arabidopsis, although positive regulation of *AG* had been well defined, characterization of its negative regulation, which is crucial for precise patterning of *AG* expression, has rather lagged behind. Negative regulators of *AG* expression, such as AP2, LEUNIG, SEUSS, and BELLRINGER, have been identified and all of them act through *AG* intron 2 (15–17). However, *cis*-elements for *AG* repression, which are the target sites for those putative transcriptional repressors, have been elusive (12, 13). Recently, binding sites for BELLRINGER were identified in *AG* intron 2 (17). These sites were, however, absent in *pMADS3* intron 2 in petunia, questioning the generality of this regulation (17). Complexes of SEUSS and SEPALLATA3 bind to the 3′ region of *AG* intron 2, thereby repressing *AG* expression (31), although the precise binding sites for this complex have not been identified (32). The TAGCT*CG*A motif in *pMADS3* intron 2 was located in the region corresponding to that including the binding site of the SEUSS-SEPALLATA3 complex in *AG* intron 2. In addition, other sequence motifs highly conserved among plant species, such as the CCAATCA boxes, were located adjacent to the TAGCT*CG*A motif (Fig. S4). This finding led us to speculate that a transcriptional repressor complex (or complexes), such as the SEPALLATA3-SEUSS complex, may interact with this region, with each component binding to a different sequence motif. Unfortunately, our attempts to verify *cis*-element activity of the TAGCTCGA motif by using a *GUS* reporter system were unsuccessful. Such experiments, however, may be possible with Arabidopsis *AG*, because *AG* intron 2 reproduces the spatiotemporal pattern of *AG* in Arabidopsis when placed upstream of the reporter gene (12). We also attempted to detect sequence-specific DNA-binding activity in nuclear extracts from petunia flowers by gel-shift assays, but TACTCGA-specific binding activity was undetectable, possibly due to technical reasons.

In RNA-induced gene activation (RNAa) in human cultured cells, small dsRNAs homologous to promoter sequences induce transcriptional activation when added to cultured cells (7, 8). Apparently, RNAa resembles the ect-*pMADS3* phenomenon in that small RNAs activate transcription. In the case of RNAa, however, significant changes were not detected in DNA methylation in the sequences targeted by small dsRNAs, but changes were detected in histone modification patterns (7). These observations obviously distinguish RNAa from the ect-*pMADS3* phenomenon, in which DNA methylation but not histone modifications is involved. Thus, the 2 phenomena are unlikely to be closely related mechanistically.

Naturally occurring epimutation has been shown to have significant effects on plant growth and development. For example, an epiallele of *Lcyc* gene in *Linaria vulgaris* is silenced due to DNA methylation, resulting in the alteration of floral symmetry (33). DNA methylation in promoter sequences silenced the *LeSPL-CNR* gene in the tomato, resulting in repressed ripening of tomato fruits (34). Paramutation of the *b1* locus in maize is another example of a naturally occurring epiallele (35). It has previously been observed in tobacco that TGS of a marker gene was inherited independent of RNA triggers, representing an artificially generated epiallele (36). The heritability of these epigenetic traits is usually based on DNA methylation of maintenance methylation sites. Presumably, RNA triggers are also involved in the generation of some, if not all, naturally occurring epialleles, as is the case of the *b1* paramutation (6). The ect-*pMADS3* phenotype is due to DNA methylation of maintenance methylation site(s) and is heritable over generations. Although it is an artificially induced one, the same could occur in nature because RNA triggers can be generated by RdRP or by hybridization of antisense RNA transcribed from many genomic regions (37) with their corresponding sense RNA. Thus, an active epiallele for a gene that is otherwise silent can be generated in nature by a mechanism similar to that involved in the ect-*pMADS3* phenomenon, suggesting a potentially broader contribution of epimutations in the formation of natural variation and plant evolution. We fortuitously noticed the ect-*pMADS3* phenotype because it is easily visible, which would otherwise have been missed because of its unpredictability. This situation is reminiscent of the finding of cosuppression, which was initially recognized as unexpected color changes in petunia flowers (38, 39).

At present, we have no information regarding the generality of ect-*pMADS3*-like regulation. Requirements for its occurrence are the presence of maintenance methylation sites in negative *cis*-elements of transcription and the generation of RNA triggers for them, which do not seem to be rare.

Materials and Methods

Plant Materials. Wild-type petunia, *P. hybrida* cv. V26 (pure line), *P. hybrida* cv. Mitchell (pure line), *P. hybrida* cv. Surfinia Purple Mini (F_1 hybrid), and transgenic petunia plants were grown under standard greenhouse conditions in a commercial potting medium.

Generation of IR Constructs and Plant Transformation. Fragments of *pMADS3* intron 2 corresponding to the regions shown in Fig. 1*A* were amplified by PCR with the primer sets listed in Table S2. The PCR fragments were cloned in sense and antisense orientation downstream of the *CaMV 35S* promoter and upstream of the *octopin synthase* terminator in a cloning vector, with a fragment of *GUS* (372 bp) inserted between the sense and antisense sequences as a spacer. These synthetic genes were cloned into the pBINPLUS (40) binary transformation vector and the resulting chimeric constructs were introduced into *P. hybrida* cv. V26 by means of *Agrobacterium tumefaciens* (GV3101)-mediated transformation (41). After regeneration on a selective medium, transformed petunia lines were transferred to a glasshouse.

Quantitative Real-time RT-PCR. Total RNA was isolated by using Trizol reagents (Invitrogen) and treated with cloned DNase I (takara Bio). Synthesis of cDNA was carried out with Oligo-dT primers by using SuperScript II reverse transcriptase (Invitrogen). PCRs were performed by using SYBR Premix ExTaq (takara Bio) with a Thermal Cycler Dice real time PCR system (Takara). To normalize the data, transcript levels of target genes relative to those of the *elongation factor* gene as an internal control were calculated. The primers for *pMADS3* were MD-c614F-RT (5′-CAAAATCCGAGCCAAAAAGA-3′) and MD-c761R-RT (5′-CCCAGGCATCAAGTTCATCT-3′), and those for *EF* were EF-F1-RT (5′-ACCACTGGTGGTTTTGAAGC-3′) and EF-R1-RT (5′-GGGTGGTAGCATCCATCTTG-3′).

Analysis of DNA Methylation. Genomic DNA was extracted with DNeasy plant mini kit (Qiagen). One microgram of DNA was digested by EcoRI, treated with Proteinase K, and cleaned up by using Wizard DNA Clean-Up systems (Promega). Bisulfite treatment was performed by using BisulFast DNA modification kit (Toyobo) according to the manufacturer's instruction. PCR reactions were performed as described by Mishiba *et al*. (42). Primers for the PCR reactions were MI-1482F-Bs (5′-GGYTGYTGAAAATGGAYGGTTG-3′) and MI-1894R-Bs (5′-CAATCTRTCTACTCAAACATRACATTRA-3′). The amplified PCR fragments were gel-purified and cloned into pGEM-T easy vector (Promega), and then 9–12 independent clones were sequenced.

ACKNOWLEDGMENTS. We thank Sumiko Tatsumi and Tomiko Yasuhara for technical assistance. This work was supported by a Grant-in-Aid for Scientific Research (to H.T.) and a Research Fellowship for Young Scientists (to K.S.) from the Japan Society for the Promotion of Science.

1. Mette MF, Aufsatz W, van der Winden J, Matzke MA, Matzke AJ (2000) Transcriptional silencing and promoter methylation triggered by double-stranded RNA. *EMBO J* 19:5194–5201.
2. Matzke MA, Birchler JA (2005) RNAi-mediated pathways in the nucleus. *Nat Rev Genet* 6:24–35.
3. Morris KV, Chan SW, Jacobsen SE, Looney DJ (2004) Small interfering RNA-induced transcriptional gene silencing in human cells. *Science* 305:1289–1292.
4. Ting AH, Schuebel KE, Herman JG, Baylin SB (2005) Short double-stranded RNA induces transcriptional gene silencing in human cancer cells in the absence of DNA methylation. *Nat Genet* 37:906–910.

5. Alleman M, *et al.* (2006) An RNA-dependent RNA polymerase is required for paramutation in maize. *Nature* 442:295–298.
6. Chandler VL (2007) Paramutation: From maize to mice. *Cell* 128:641–645.
7. Li LC, *et al.* (2006) Small dsRNAs induce transcriptional activation in human cells. *Proc Natl Acad Sci USA* 103:17337–17342.
8. Janowski BA, *et al.* (2007) Activating gene expression in mammalian cells with promoter-targeted duplex RNAs. *Nat Chem Biol* 3:166–173.
9. Kapoor M, *et al.* (2005) Transgene-triggered, epigenetically regulated ectopic expression of a flower homeotic gene *pMADS3* in *Petunia*. *Plant J* 43:649–661.
10. Tsuchimoto S, van der Krol AR, Chua NH (1993) Ectopic expression of *pMADS3* in transgenic petunia phenocopies the petunia blind mutant. *Plant Cell* 5:843–853.
11. Sieburth LE, Meyerowitz EM (1997) Molecular dissection of the AGAMOUS control region shows that cis elements for spatial regulation are located intragenically. *Plant Cell* 9:355–365.
12. Busch MA, Bomblies K, Weigel D (1999) Activation of a floral homeotic gene in Arabidopsis. *Science* 285:585–587.
13. Deyholos MK, Sieburth LE (2000) Separable whorl-specific expression and negative regulation by enhancer elements within the AGAMOUS second intron. *Plant Cell* 12:1799–1810.
14. Lohmann JU, *et al.* (2001) A molecular link between stem cell regulation and floral patterning in Arabidopsis. *Cell* 105:793–803.
15. Liu Z, Meyerowitz EM (1995) LEUNIG regulates AGAMOUS expression in Arabidopsis flowers. *Development* 121:975–991.
16. Franks RG, Wang C, Levin JZ, Liu Z (2002) SEUSS, a member of a novel family of plant regulatory proteins, represses floral homeotic gene expression with LEUNIG. *Development* 129:253–263.
17. Bao X, Franks RG, Levin JZ, Liu Z (2004) Repression of AGAMOUS by BELLRINGER in floral and inflorescence meristems. *Plant Cell* 16:1478–1489.
18. Metzlaff M, O'Dell M, Hellens R, Flavell RB (2000) Developmentally and transgene regulated nuclear processing of primary transcripts of *chalcone synthase A* in petunia. *Plant J* 23:63–72.
19. O'Dell M, Metzlaff M, Flavell RB (1999) Post-transcriptional gene silencing of chalcone synthase in transgenic petunias, cytosine methylation and epigenetic variation. *Plant J* 18:33–42.
20. Sarraf SA, Stancheva I (2004) Methyl-CpG binding protein MBD1 couples histone H3 methylation at lysine 9 by SETDB1 to DNA replication and chromatin assembly. *Mol Cell* 15:595–605.
21. Johnson LM, *et al.* (2007) The SRA methyl-cytosine-binding domain links DNA and histone methylation. *Curr Biol* 17:379–384.
22. Schubert D, *et al.* (2006) Silencing by plant Polycomb-group genes requires dispersed trimethylation of histone H3 at lysine 27. *EMBO J* 25:4638–4649.
23. Hong RL, Hamaguchi L, Busch MA, Weigel D (2003) Regulatory elements of the floral homeotic gene AGAMOUS identified by phylogenetic footprinting and shadowing. *Plant Cell* 15:1296–1309.
24. Petersen BO, Albrechtsen M (2005) Evidence implying only unprimed RdRP activity during transitive gene silencing in plants. *Plant Mol Biol* 58:575–583.
25. Kinoshita Y, *et al.* (2007) Control of *FWA* gene silencing in Arabidopsis thaliana by SINE-related direct repeats. *Plant J* 49:38–45.
26. Bernstein BE, Meissner A, Lander ES (2007) The mammalian epigenome. *Cell* 128:669–681.
27. Deng G, Chen A, Pong E, Kim YS (2001) Methylation in *hMLH1* promoter interferes with its binding to transcription factor CBF and inhibits gene expression. *Oncogene* 20:7120–7127.
28. Kapoor M, *et al.* (2002) Role of petunia pMADS3 in determination of floral organ and meristem identity, as revealed by its loss of function. *Plant J* 32:115–127.
29. Eden S, *et al.* (2001) An upstream repressor element plays a role in Igf2 imprinting. *EMBO J* 20:3518–3525.
30. Murrell A, *et al.* (2001) An intragenic methylated region in the imprinted *Igf2* gene augments transcription. *EMBO Rep* 2:1101–1106.
31. Sridhar VV, Surendrarao A, Gonzalez D, Conlan RS, Liu Z (2004) Transcriptional repression of target genes by LEUNIG and SEUSS, two interacting regulatory proteins for Arabidopsis flower development. *Proc Natl Acad Sci USA* 101:11494–11499.
32. Sridhar VV, Surendrarao A, Liu Z (2006) APETALA1 and SEPALLATA3 interact with SEUSS to mediate transcription repression during flower development. *Development* 133:3159–3166.
33. Cubas P, Vincent C, Coen E (1999) An epigenetic mutation responsible for natural variation in floral symmetry. *Nature* 401:157–161.
34. Manning K, *et al.* (2006) A naturally occurring epigenetic mutation in a gene encoding an SBP-box transcription factor inhibits tomato fruit ripening. *Nat Genet* 38:948–952.
35. Stam M, Belele C, Dorweiler JE, Chandler VL (2002) Differential chromatin structure within a tandem array 100 kb upstream of the maize b1 locus is associated with paramutation. *Genes Dev* 16:1906–1918.
36. Jones L, Ratcliff F, Baulcombe DC (2001) RNA-directed transcriptional gene silencing in plants can be inherited independently of the RNA trigger and requires Met1 for maintenance. *Curr Biol* 11:747–757.
37. Stolc V, *et al.* (2005) Identification of transcribed sequences in Arabidopsis thaliana by using high-resolution genome tiling arrays. *Proc Natl Acad Sci USA* 102:4453–4458.
38. Napoli C, Lemieux C, Jorgensen R (1990) Introduction of a chimeric *chalcone synthase* gene into petunia results in reversible co-suppression of homologous genes in trans. *Plant Cell* 2:279–289.
39. van der Krol AR, Mur LA, Beld M, Mol JN, Stuitje AR (1990) Flavonoid genes in petunia: addition of a limited number of gene copies may lead to a suppression of gene expression. *Plant Cell* 2:291–299.
40. van Engelen FA, *et al.* (1995) pBINPLUS: An improved plant transformation vector based on pBIN19. *Transgenic Res* 4:288–290.
41. Jorgensen RA, Cluster PD, English J, Que Q, Napoli CA (1996) Chalcone synthase cosuppression phenotypes in petunia flowers: Comparison of sense vs. antisense constructs and single-copy vs. complex T-DNA sequences. *Plant Mol Biol* 31:957–973.
42. Mishiba K, *et al.* (2005) Consistent transcriptional silencing of 35S-driven transgenes in gentian. *Plant J* 44:541–556.